Performance evaluation of DTM Area-based matching reconstruction of Moon and Mars

Cristina Re[1], Gabriele Cremonese[3], Elisa Dall'Asta[2], Gianfranco Forlani[2], Giampiero Naletto[4], Riccardo Roncella[2]

[1]Centro Interdipartimentale Studi e Attività Spaziali (CISAS)–G. Colombo, University of Padova;
[2]Dept. of Civil Engineering, University of Parma, Italy;
[3]INAF - Astronomical Observatory, 35122 Padova Italy;
[4]Department of Information Engineering, University of Padova, Italy

ABSTRACT

High resolution DTMs, suitable for geomorphological studies of planets and asteroids, are today among the main scientific goals of space missions. In the framework of the BepiColombo mission, we are experimenting the use of different matching algorithms as well as the use of different geometric transformation models between stereo pairs, assessing their performances in terms of accuracy and computational efforts. Results obtained with our matching software are compared with those of established software. The comparison of the performance of image matching being the main objective of this work, all other steps of the DTM generation procedure have been made independent of the matching software by using a common framework. Tests with different transformation models have been performed using computer generated images as well as real HiRISE and LROC NAC images. The matching accuracy for real images has been checked in terms of reconstruction error against DTMs of Mars and the Moon published online and produced by the University of Arizona.

Keywords: Space Photogrammetry**,** DTM Reconstruction Accuracy, Area-based Image Matching, Image Warping

1. INTRODUCTION

The BepiColombo space mission is a joint effort of the European Space Agency (ESA) and of the Japanese Space Agency (JAXA): ESA Mercury Planetary Orbiter and JAXA Mercury Magnetospheric Orbiter will be launched in August 2015 to Mercury to study the surface composition and morphology, the geology and the magnetosphere of the innermost Planet of the Solar System. ESA MPO spacecraft will support remote sensing and radio-science instrumentation and will host the Spectrometer and Imagers for MPO BepiColombo Integrated Observatory SYStem (SIMBIO-SYS). The SIMBIO–SYS suite [1] has been designed as an integrated package of different channels mounted on a common optical bench. The suite includes an imaging system with stereo (STC) [2] and high spatial resolution (HRIC) capabilities along with a hyper spectral imager (VIHI) in the visible-near infrared range. The instrument development is based on the joint efforts of Italy and France, with Selex Galileo S.p.A as industrial partner. The STC main scientific objective is the global mapping of the planet with stereo imaging with ground pixel resolution of 50 m at the equator and 110 m at the poles; with image measurement accuracy of 1 pixel, the vertical accuracy of object points at periherm is expected to be 84 m.

Algorithms and software for Digital Terrain Models (DTM) generation from STC images are being developed. Tests are currently performed with the program Dense Matcher (DM) [3] of the University of Parma, applying an area-based method with subpixel accuracy, the Least Squares Matching (LSM) [4]. In [5] early results of DM on DTM generation from synthetic STC images were shown; this paper presents the latest results of an investigation with computer-generated images as well as HiRISE [6] and LROC NAC [7] images, where several matching parameters have been varied to study their effect on matching accuracy. In addition to the standard affine transformation normally used in the

LSM algorithm, other geometric transformations have also been tested and results will be shown on both computer-generated and real images.
The accuracy of the DTM reconstruction and the percentage of good matches obtained are evaluated to assess the performance of DM. To this aim, for tests with real space images, the 3D reconstruction results of DM are compared with those obtained by the software package Ames Stereo Pipeline (ASP) [8], using as reference data DTMs of Mars and the Moon produced by the University of Arizona with Socet Set®.

2. IMAGE MATCHING ALGORITHMS

A large number of area-based methods have been developed to search for image correspondences [9]: it is out of the scope of this paper to review the topic; here just two will be briefly described, that have been used for DTM generation in this test: the NCC (Normalized Cross Correlation) [10] and the Least Squares Matching (LSM). Though very basic and bound by several hypotheses, the former is still widely used, often in combination with some pre-processing step to rectify the images and improve the similarity of the patches. To the contrary, the latter uses two simple mathematical models (see 2.2) to describe the geometric and radiometric differences between the image patches; estimation of the parameters of these models in a least-squares adjustment drives the resampling of the search image to minimize the squared sum of the grey values differences between template and patch.

2.1 NCC

The NCC algorithm looks for similarities between images by shifting a reference window over a search image and computing at each position the Normalized Cross Correlation coefficient:

$$\mathrm{NCC} = \frac{\sigma_{12}}{\sigma_1 \sigma_2} \frac{\sum_{r=1}^{R}\sum_{c=1}^{C}(g_1(r,c)-\mu_1)\cdot(g_2(r,c)-\mu_2)}{\sqrt{\sum_{r=1}^{R}\sum_{c=1}^{C}(g_1(r,c)-\mu_1)^2 \cdot \sum_{r=1}^{R}\sum_{c=1}^{C}(g_2(r,c)-\mu_2)^2}} \tag{1}$$

where:

$g_1(r,c)$, $g_2(r,c)$ = reference and search window, both of size (R,C)

μ_1 , μ_2, σ_1, σ_2 = grey values averages and standard deviations in the two windows

σ_{12} = covariance between the grey values of the two windows

Ideally, the unit value for the correlation coefficient can only be obtained by a noise-free image pair of a flat surface with images acquired in the so called normal case of photogrammetry. In practice, unless these conditions are approximately met, pre-processing of images is necessary. Several efficient implementation tricks can be used to improve speed and reduce the computational burden for the search of the homologous [10]; sub pixel accuracy can be achieved if the correlation coefficients in a window around the maximum are interpolated by a smooth polynomial function, so that the position of the maximum is derived analytically from the function coefficients.

2.2 LSM

The LSM [4] uses an explicit modeling of radiometric and geometric differences between images to minimize the grey values differences between template and patch; to keep the overall model simple but still effective, in most implementations the radiometric parameters allow a linear contrast stretch while the geometric parameters allow an affine transformation between the two images. The affine model is an approximation of the actual transformation between the two images, even when the object surface in the search area can be assumed to be flat; however, for small patches and not too convergent images it works generally well. Given two corresponding image patches *g(x,y)* and *f(u,v)*, accounting for image noise *n(x,y)* and for a linear radiometric transformation with parameters r_0, r_1 we can write:

$$g(x, y) = r_0(x,y) + r_1(x,y)\, f\,(u(x,y), v(x,y)) + n(x, y) \tag{2}$$

where

$$u(x,y) = a_0 + a_1 x + a_2 y \qquad\qquad v(x,y) = b_0 + b_1 x + b_2 y \tag{3}$$

is the affine (AFF in the following) transformation that links the homologous pixels locally (i.e. within the template). The convergence radius of LSM is relatively small (a few pixels): therefore a good approximation of the disparity map is necessary to initialize the process. The main parameters to set in the processing are the threshold on the correlation coefficient to accept the match as successful and the template size. Linearization of (2) with respect to the parameters (a_0, ..., b_2) requires the computation of the derivatives of the grey values with respect to *(u,v)* using numerical approximations. In case some of the parameters in (3) are constrained or omitted, simpler geometric models can be implemented. In the following, SHIFT refers to the case when only the parameters a_0 and b_0 are used; in this form the LSM model is basically equivalent to a sub-pixel NCC implementation, the difference being the search of the maximum.

In a recent paper [11] it has been proposed to extend the functional model of the geometric transformation of the LSM in order to improve the capability of the method when images are convergent and/or the object cannot be considered to be flat within the template. The motivation for this is to implement a more accurate or realistic modeling of the map between the two images, trying to overcome the limitations of the AFF model when its assumptions (especially along terrain edges) are not met. Two extended functional models have been suggested; the first aims specifically at convergent image pairs, the second is meant to improve the implicit modeling of the object shape with rough terrain.

If the object is flat within the template window, the relationship between the images is a (non linear) projective transformation (PROJ in the following) that depends on 8 parameters:

$$u(x,y)= \frac{a_0 + a_1 x + a_2 y}{1 + c_1 x + c_2 y} \qquad v(x,y)= \frac{b_0 + b_1 x + b_2 y}{1 + c_1 x + c_2 y} \tag{4}$$

If the object is not flat within the template window, modelling the relationship between the two images requires knowledge of the object shape; however, a polynomial (POLY in the following) function of low order can be applied:

$$u(x,y)= \sum_{j=0}^{n} \sum_{i=o}^{j} a_{ji} \cdot x^{j-i} \cdot y^{i} \qquad v(x,y)= \sum_{j=0}^{n} \sum_{i=o}^{j} b_{ji} \cdot x^{j-i} \cdot y^{i} \tag{5}$$

Using such a model, on a real image pair of a curved object a fourfold accuracy increase in DTM reconstruction has been reported in [11] when using POLY rather than AFF.

An experimental evaluation of these extended models has been performed using synthetic and real images: its results are shown in Sections 4 and 5; in particular, model (5) has been used with a 2nd degree polynomial (12 parameters overall).

3. IMAGE MATCHING SOFTWARE USED IN THE TESTS

3.1 Dense Matcher

The DTM generation program Dense Matcher [3] of the University of Parma implements three matching methods: NCC, LSM and the Multiphoto Geometrically Constrained Matching (MGCM) [12]; in a beta release, besides NCC and AFF, also SHIFT, PROJ and POLY modes are available. The matching stage can be embedded in a multi-resolution approach where three levels of an image pyramid are processed. An initial disparity map can be computed using feature based matching (SURF [13]) followed by interpolation of the accepted disparities on a regular grid using a Delaunay triangulation. A NCC matching step can be executed to improve the initial disparity map (optionally at each level of the pyramid); afterwards the LSM algorithm is applied to refine the disparity with a parallel dense matching procedure. Epipolar resampling can be applied to improve efficiency and computational speed. To control the processing, use of image pyramids, the acceptance threshold for the correlation coefficient between the g.v. of template and patch, the template size, the pixel spacing between template centers can be set. No hole-filling or other post-processing on the final disparity map is currently performed.

3.2 Ames Stereo Pipeline

The image matching program ASP is “an open source suite of fully automated geodesy and stereogrammetry tools designed to process planetary imagery captured from robotic explorers” [14] from the NASA Ames Intelligent Robotics Group. The program is integrated with the updated versions of USGS ISIS software package [15] that is now a standard for processing, analyzing and archiving images and ancillary information of NASA space missions. An exaustive

documentation on ASP features, references and a user guide can be found in [16]; as far as image matching is concerned, two modes are available: SUB_PIXEL_MODE 1 fits a parabolic surface to the NCC values of the 8-connected neighborhood of the "best" NCC value while SUB_PIXEL_MODE 2 uses an affine-adaptive deformable template whose parameters are treated as random variables in a Bayes Expectation Maximization framework that allows robustness to image noise; this has strong similarities with the affine model of LSM.

4. DESCRIPTION OF THE TESTS

The tests on matching accuracy have been organized in three stages; in the first (STAGE 1), real HiRISE images have been processed with both DM and ASP and compared to the reference DTM of the University of Arizona; in the second one (STAGE 2) all the functional models of LSM described in Section 2 and the NCC have been applied to synthetic images only, to get a preliminary evaluation of their performance under controlled and ideal conditions; in the third one (STAGE 3) the same functional models have been applied to LROC NAC images processed with DM and compared to the results of ASP and to the reference DTM from University of Arizona. In the following, more details will be provided for each stage; finally, the procedure used for the comparison of the results will be presented.

4.1 STAGE 1: DTM generation with LSM affine model on HiRISE images

The goal of this stage was to compare the performance of DM with more established software. A stereo pair of HiRISE images in Melas Chasma basin has been retrieved from the HiRISE website (http://hirise.lpl.arizona.edu) together with the corresponding DTM. Image PSP_008669_1705 has been acquired on 2008/06/01 with a 26.6 cm/pixel resolution and phase angle of 63.6°. Image PSP_009025_1705 has been acquired on 2008/06/29 with a resolution of 26.7 cm/pixel and a phase angle of 52.7°. According to the header cube data file, the reference DTM (DTEEC_008669_1705_009025_1705_A01) has been produced by A. McEwen and Sarah Mattson of the University of Arizona using SocetSet® from BAE Systems. Of the whole image, results on an image crop of about 2000x2000 pixels (see Figure 1, left) will be shown in Section 5. Image matching has been performed with both DM and ASP by varying the template size from 9 to 25 pixels; DM performed the LSM with the affine transformation model (AFF) while in ASP SUB_PIXEL_MODE 2 has been used.

4.2 STAGE 2: DTM generation with different LSM transformation functions from computer-generated images

To test the performance of the different transformation functions in the LSM under ideal conditions, synthetic images were generated using a 3D modeler. With this program, a 3D model of an object can be imported and draped with a texture; then, virtual cameras can be created and placed in the scene, setting the illumination sources; finally, images taken by the cameras can be generated and exported in common image formats. Two types of object surfaces have been considered: a plane surface (case *plane*) and a sample of a topographic surface (case *DTM*), taken from a patch of the Mars reference DTM used in Stage 1. The images were produced both in the normal case (nadir images, with no relative rotations between the two camera systems) as well as with convergent views, with an angle between the camera axes close to 20°. Two artificial patterns available in the 3D modeler library (*cellular* and *asphalt*, see Figure 2) have been overlaid on the reference objects; in addition, for the Mars DTM patch only, synthetic images were also generated projecting the real HiRISE image texture. No image noise has been added to the grey values.
Using such synthetic images and their known exterior and interior orientation parameters, a point cloud is generated by image matching followed by triangulation; the reconstruction error in object space is evaluated point-wise as the distance of each matched point from the reference DTM. The functional models NCC, SHIFT, AFF, PROJ and POLY have been used varying texture, template size, base-to-height ratio, max number of iterations and matching acceptance threshold.

4.3 STAGE 3: DTM generation with different functional models on LROC NAC images

In the last stage, all the above functional models have been applied to LROC NAC images with DM; in parallel, ASP has been executed with SUB_PIXEL_MODE 1 and 2, i.e. with functional models very similar to NCC and AFF models. Also in these tests template size, max number of iterations, threshold for the correlation coefficient have been varied. A stereo pair of LROC images near the Moore crater (37.3° latitude,185.0° longitude) has been retrieved from the LROC website (http://www.lroc.asu.edu) together with the corresponding DTM. Both have been acquired on 2010/04/12 a few hours apart; image M125720601LE has 55.7 cm/pixel resolution and a phase angle is 42°, while image M125713813LE has a resolution of 59 cm/pixel and a phase angle of 34.6°. According to the header cube data file, the DTM used as

reference (NAC_DTM_MOOREF1_E370N1850) has been produced by Mark Robinson of the University of Arizona using SocetSet®. Of the whole image, results on just a patch of about 2300x2300 pixels will be shown.

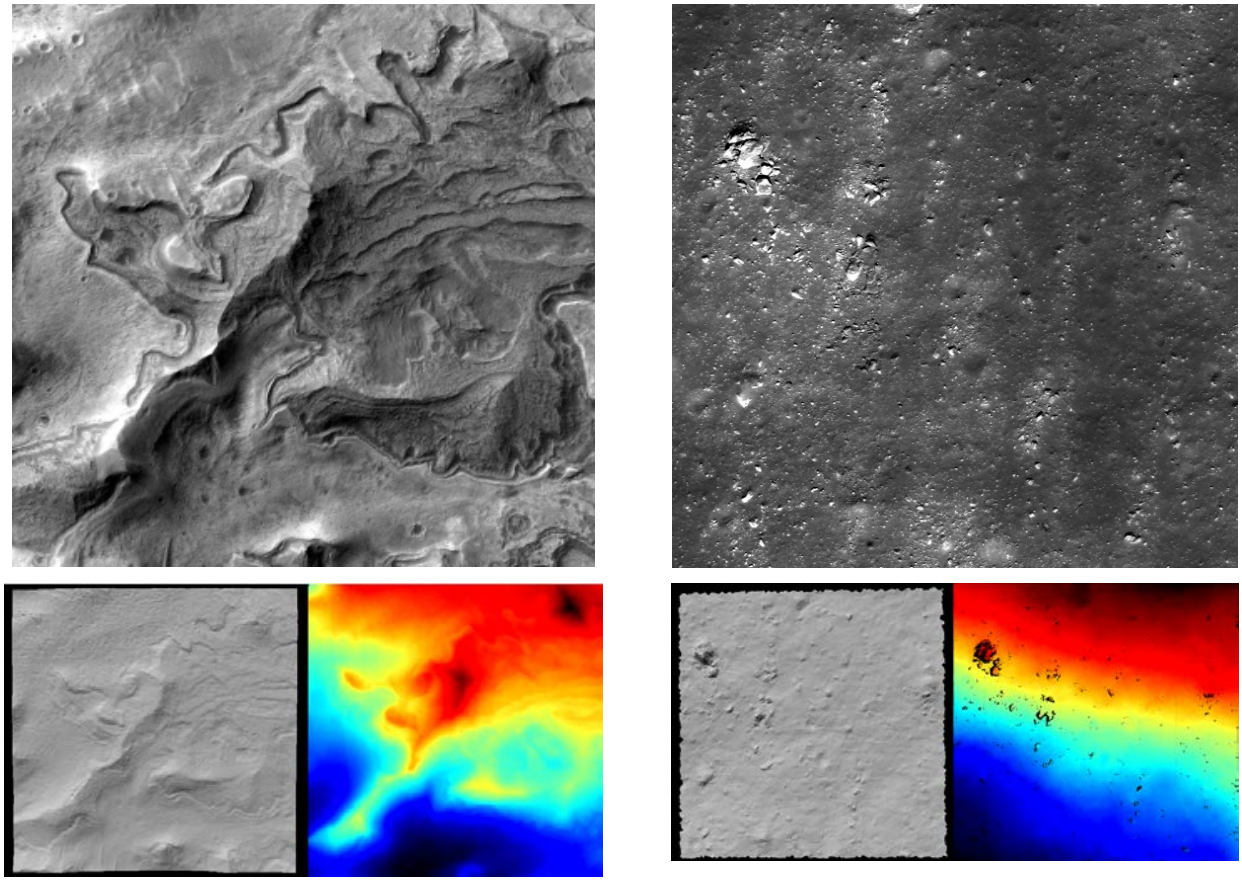

Figure 1. Test Stage 1 and 3: left: the HiRISE PSP_009025_1705 image patch processed, approximately 520x520 m wide; below a shaded relief and a color coded DTM visualization; right: the LROC NAC M125713813LE image patch processed, approximately 1300x1300 m wide; below a shaded relief and a color coded DTM visualization.

Figure 2. Test stage 2: texture patterns used in the synthetic images: left: *cellular*; centre: *asphalt*; right: *Mars*.

4.4 DTM generation and comparison procedure

As far as the real images are concerned, preprocessing steps have been performed with ISIS; in particular, both HiRISE and LROC NAC images were initially map-projected using the ISIS function cam2map. The objective of the test being the matching accuracy, either possible differences due to the triangulation to compute the ground coordinates as well as systematic deviations due to discrepancies in the exterior orientation parameters available were considered. As far as

triangulation is concerned, the ASP framework has been used by suitably modifying the DM output to produce the input data in the format accepted by ASP. Figure 3 shows the modified ASP flow-chart where, after preprocessing, the image matching engine of ASP or of DM is activated to produce the refined disparity map; after outlier rejection, the triangulation provides the object coordinates for DTM generation and the mesh for visualization.

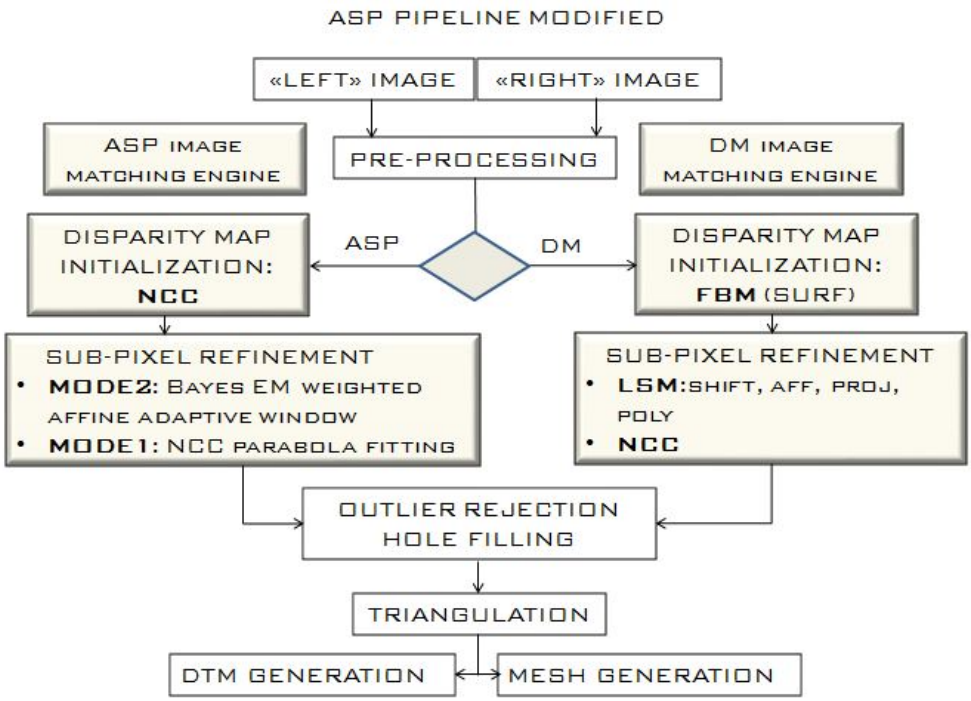

Figure 3. Processing of HiRISE and LROC NAC images (Stages 1 and 3): ASP DTM generation flow-chart modified to accommodate either the ASP or the DM image matching engine to produce the refined disparity map

To reduce as far as possible deviations from the produced DTM and the reference DTM due to discrepancies between the exterior orientation parameters available in the cub files and those used by University of Arizona, each DTM produced by DM or ASP has been aligned to the reference DTM with a surface-to-surface matching procedure; the results in Section 5 therefore refers to the discrepancies between the aligned DTMs. To compute the discrepancies, the reference data sets have been converted to a TIN representation and compared to the triangulated point cloud generated by DM and ASP. The signed distance of each point to the triangulated reference surface is the error measure that has been considered; the RMSE therefore refers to such distances. In addition, the number of accepted matches based on the correlation threshold is reported.

5. RESULTS

5.1 Stage 1

The DTM of the HiRISE image patch shown in Figure 1 has been generated with different template sizes; an acceptance threshold of 0.8 and the AFF model have been used with DM, SUBPIXEL_MODE_2 with ASP. Table 1 shows the RMSE error and the number of good matches of ASP and DM with template size 9x9 and 25x25. As far as the accuracy is concerned, DM and ASP show similar performances, with ASP better with larger templates and DM better with smaller ones; ASP finds about 5% more good matches. More details on the comparison and more results than those given here can be found in [3]; they suggest an overall similar performance of the two programs. As a general remark, the accuracy as well as the number of matches increases with the template size. Figure 4 shows the color error map for DM with the two templates; in the blank areas the correlation coefficient is below the threshold. Some systematic effects show up in the error pattern along vertical strips and as a fringe pattern in the lower part; the largest errors, though, occur in the steepest areas (see Figure 1, left).

Table 1. HiRISE images: RMSE and number of good matches for ASP and DM with two different templates.

	RMSE (cm)	**# matches**		**RMSE (cm)**	**# matches**
ASP_T25	16.4	5074000	DM_T25	17.7	4904000
ASP_T09	25.8	4998000	DM_T09	21.6	4709000

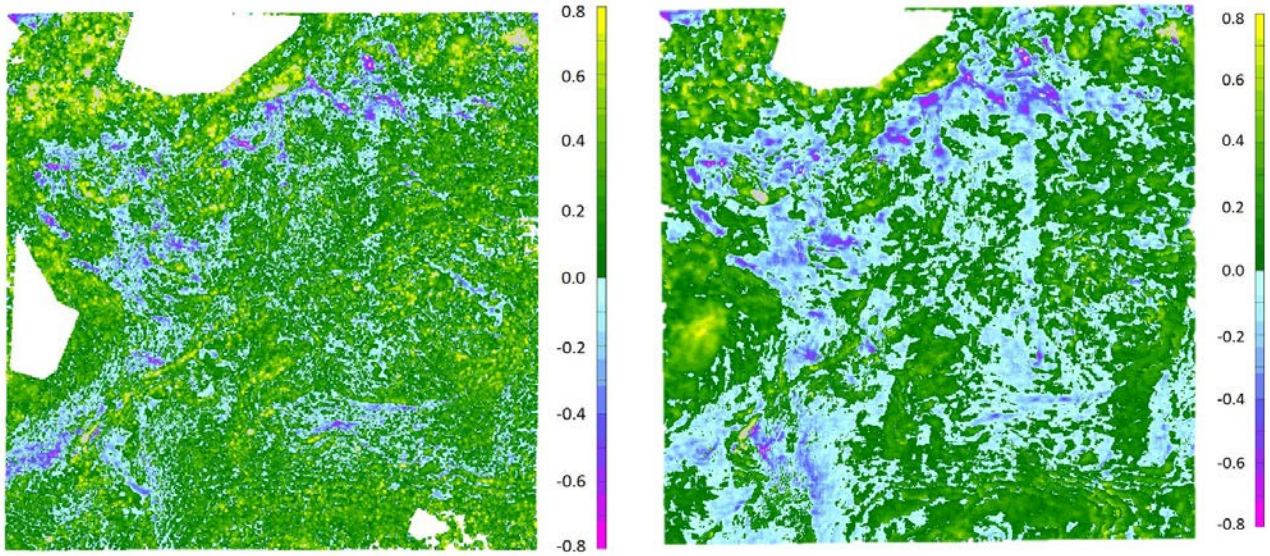

Figure 4. HiRISE images: color error map of DM with respect to the reference DTM (AFF): left: template 9; right: template 25. Areas where the acceptance threshold (0.8) is not satisfied are left blank

5.2 Stage 2

A large number of tests have been executed and their results cannot be fully shown here. The following graphs refer to the RMSE of the elevation for points accepted with a correlation coefficient threshold of 0.9, a base-to-height ratio of 1:5.8 and *asphalt* or *Mars* texture. The elevation accuracy unit of measurement (unspecified) is the same for all graphs. Figure 5 shows the results for the surface *plane* with texture *asphalt* and nadir or convergent images. In the nadir case for all methods accuracy improves with template size, though with different rates; a clear minimum cannot be identified; the complex the mathematical model, the poorer the accuracy for small templates. SHIFT, which is theoretically the correct geometric transformation model, has the smallest accuracy range: from 0.54 to 0.31; AFF has the same trend as SHIFT, but only from templates larger than 17, and the best overall accuracy value (0.24). NCC accuracy ranges from 1.88 to 0.57. PROJ has a trend very similar to AFF, but it is slightly less accurate (best value 0.28) and needs larger templates to have good results. The same applies also to POLY, but the accuracy is not as good, with a best value of 0.49.

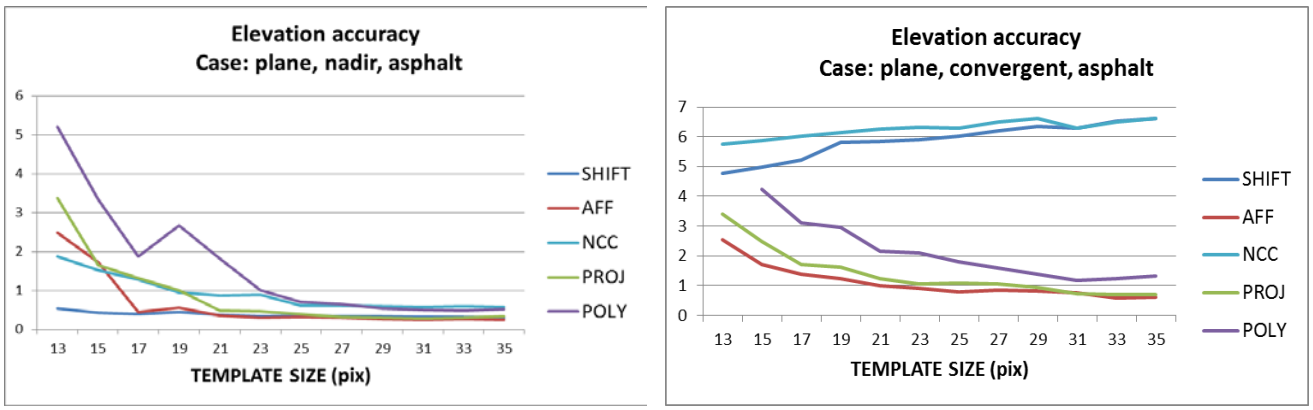

Figure 5. Elevation accuracy with plane surface, asphalt texture and nadir (left) or convergent (right) images with SHIFT, AFF and NCC models

With convergent images (correct model: PROJ) only AFF, PROJ and POLY are able to accommodate to some extent the perspective differences, with again accuracy improving with template size and no clear minimum reached. Compare to the previous case the accuracy is poorer (best value for AFF 0.59); AFF is about 20% better than PROJ and two times better than POLY. NCC and SHIFT do not provide good results and their accuracy gets worse with template size.
Figure 6 summarizes the results with nadir and convergent images and with *asphalt* and *Mars* textures for the object *DTM*. The trends of the various models with template size are less clear; image texture matters with convergent images, with *asphalt* easier to match than *Mars*. Again, SHIFT and NCC cannot properly model the perspective differences; their accuracy is worse than with *plane* and degrades with template size. The trend for AFF shows a minimum, more pronounced with nadir images, that is reached in the interval 19-21 template size. Compared to the best results with *plane* (0.24), *DTM* is a more difficult case: the best accuracy is 1.11 with *asphalt* and 1.47 with *Mars* texture.
PROJ also shows a minimum with the template size in the interval 21-25 pixels, depending on object texture and on whether nadir or convergent images are used. As far as POLY is concerned, there is an increase in accuracy with template size; a minimum (an optimal template size) is more difficult to identify than for AFF and PROJ, but is most likely for larger template sizes than AFF and PROJ.
As can be expected, convergent images are more demanding than nadir images: for both PROJ and POLY the best accuracy value is about two times better with nadir ones. Overall, from the cases presented, there is not a clear advantage in using PROJ rather than AFF: with *asphalt* the best values of AFF and PROJ are nearly the same, with *Mars* AFF is better. POLY shows no clear minimum with template size; the best values of AFF and POLY are very close in two cases out of four; in the others the accuracy gain with POLY, though, does not exceed a factor of about 1.5.

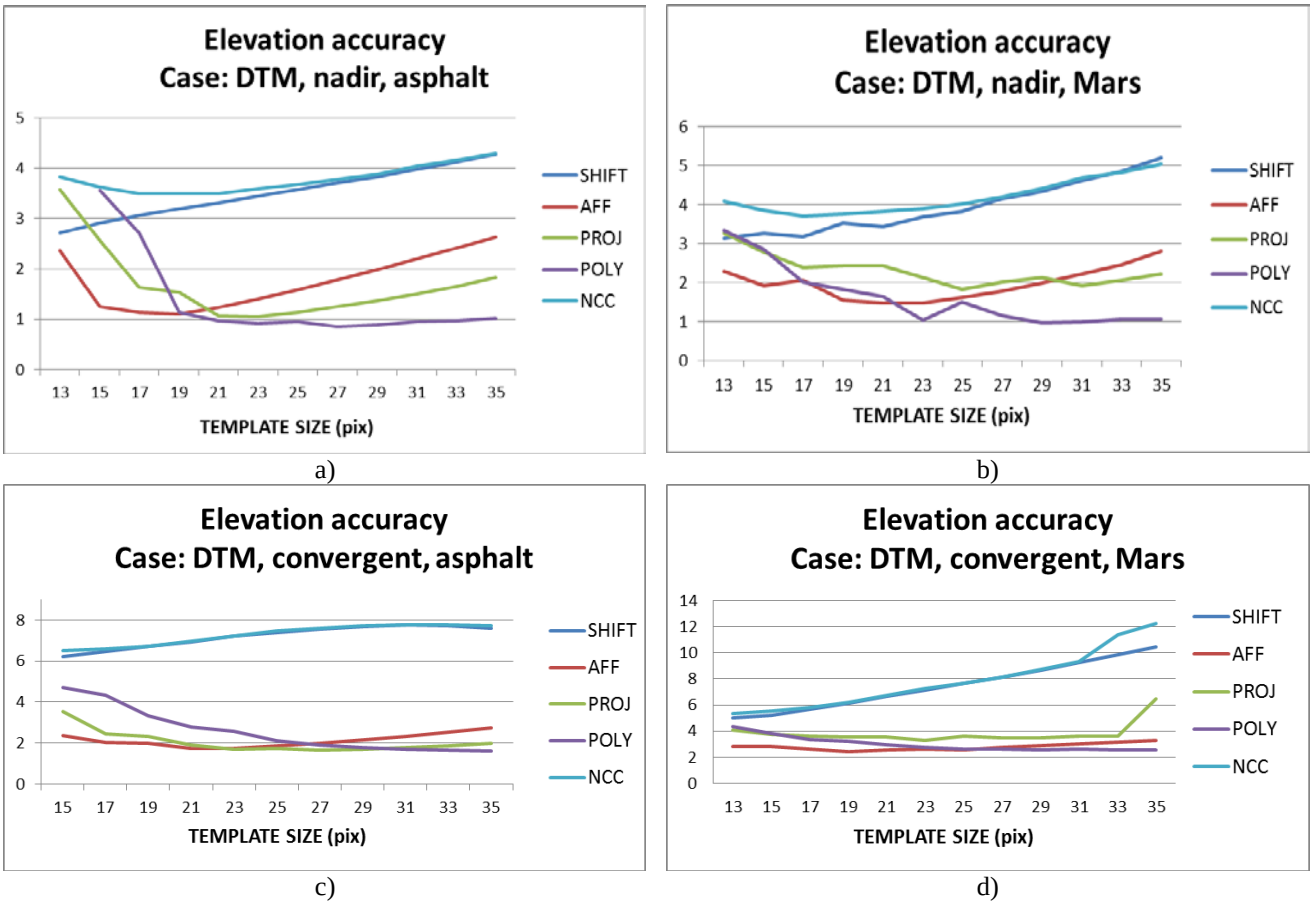

Figure 6. Elevation accuracy with DTM surface, with different texture and nadir or convergent images with all five functional models

Epipolar resampling (ER) is routinely applied in stereo matching with frame images in order to make the process more robust and speed up the matching by reducing the search space; in addition, the similarity of the images improves. It can be compared to the map-projection usually performed on stereo images obtained using a linear CCD sensor (like HiRISE

or LROC NAC). Such preprocessing step is normally performed in DM, though it has not been used in the test described above; to find out whether it affects dense matching, one of the cases has been processed also after epipolar resampling. The results are shown in Figure 7, where it can be seen that the accuracy of NCC and SHIFT is close (though slightly worse) to that of Figure 6a, i.e. to the nadir case. As far as AFF is concerned, the accuracy with ER is on average around 3 while without ER (Figure 6c) the average is about 2. This suggests that in some cases ER may help the simpler functional model to perform better but at the same time may make matters worse to more complex models. Since NCC has a computational cost that is several times smaller than AFF, whenever time is an issue, as with processing large amount of data, the choice of the matching model should be considered with care. However, it should not be forgotten that the above graphs refer to a quite selective threshold and do not show the interdependence among threshold, accuracy and number of good matches.

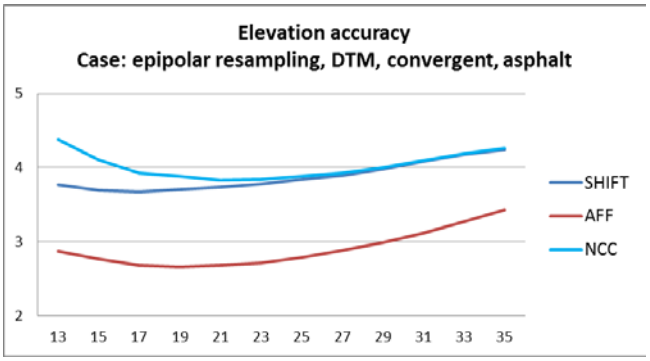

Figure 7. Elevation accuracy if dense matching is performed after epipolar resampling of images in the case of Figure 6c

5.3 Stage 3

As mentioned in Section 4.3, all functional models have been applied to LROC NAC images with DM; in parallel, ASP has been executed with SUB_PIXEL_MODE 1 and 2. The template size has been varied from 9x9 to 33x33 pixels. Figure 8 shows the comparison between DM and ASP in terms of accuracy of the DTM reconstruction and of the number of matches, as a function of the template size. DM and ASP show the same consistent trend: an increase of accuracy with the template size.

Both DM and ASP show very similar values of accuracy: within 2 cm with the AFF model and within 5 cm with NCC, with ASP providing better results and with SUB_PIXEL_MODE 1 and 2 basically equivalent in terms of accuracy. The number of good matches depends on the template size; DM has the same trend with both AFF and NCC while ASP, that finds about 13% more matches than DM with the AFF model, has a drop of performance with NCC.

AFF and NCC show substantially equivalent DTM reconstruction accuracy. For instance, NCC reaches its best accuracy with the 21x21 template, with just 4 cm accuracy gap to AFF; the best accuracy for AFF is with the 29x29 template, an accuracy 10 cm better than NCC's but at a quite different computational cost. Using NCC with map-projected images with smooth or flat terrain could be preferable, especially if we want to produce the DTM in shorter times.

The graph in Figure 9 compares the results of DM with all the functional models. As with the synthetic cases in section 5.2 there is a general improvement increasing the template size; a minimum is reached for SHIFT and NCC but not for AFF, PROJ and POLY. AFF offers the best results, with an improvement from 54 cm to 38 cm. SHIFT, NCC and PROJ show results more or less in the same range (from 56 to 45 cm) although PROJ might further improve with larger templates. POLY gets the worst results (from 59 cm to 51 cm). This is partly in contrast to what has been shown in the previous section and to the results shown in [11]; it might be a feature of POLY that requires more investigations. Possibly, estimation errors might arise due to overparametrization; indeed POLY seems to have problems with very smooth or flat surfaces such as the case *plane* with nadir images (Figure 5 left) and the Moon area of Figure 9 that looks basically an inclined plane. On the contrary the object shape in [11] has a large curvature that exploits the greater flexibility of the model.

Figure 10 shows the error color map of DM with respect to reference DTM. The left image shows the comparison relative to the Affine model and the right one the Polynomial model. Although the error maps have a very similar pattern in both cases, it is apparent that the error surface is smoother for the Affine model; moreover, the absolute errors of the Polynomial model are larger (there are more yellow and purple areas). In both DTMs, the error pattern show vertical strips where the error sign is constant.

Figure 8. LROC NAC images: elevation accuracy of the DTM produced by DM and ASP with respect to reference DTM and number of matches (AFF model and NCC model) as a function of template size

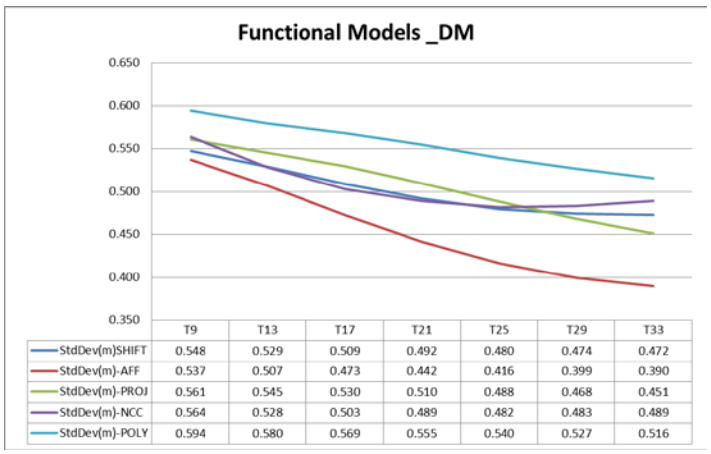

Figure 9. LROC NAC images: elevation accuracy of DM with respect to reference DTM (SHIFT, AFF, PROJ, NCC, POLY models) as a function of template size

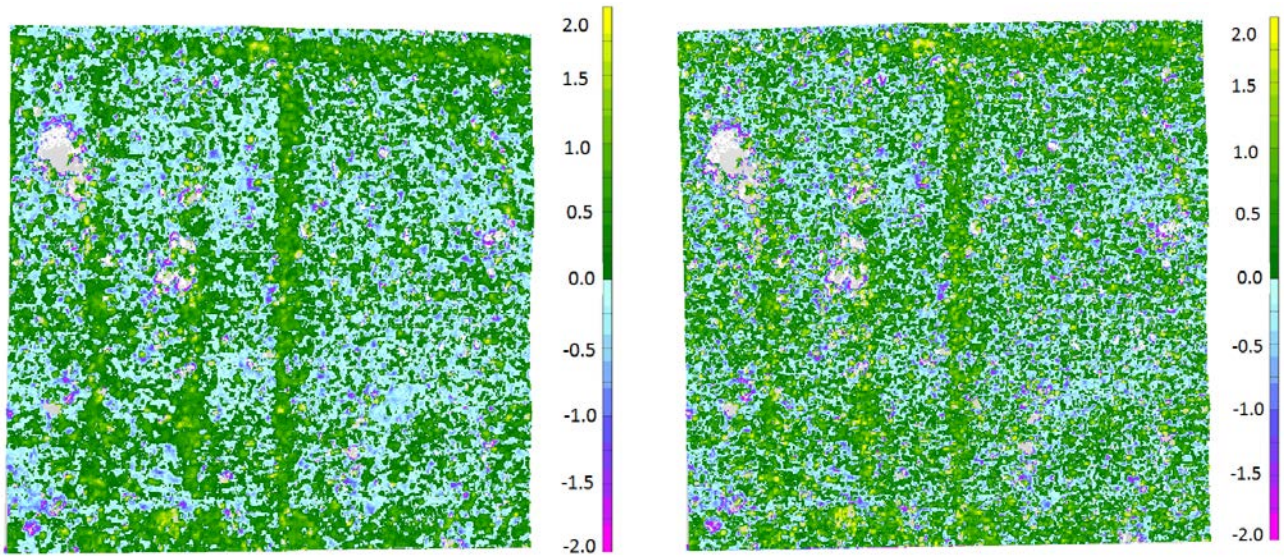

Figure 10. LROC NAC images: DM error color map of the DTM reconstruction. Left: Affine model (T21). Right: Polynomial model (T21).

6. CONCLUSIONS

A large number of tests have been conducted to investigate the accuracy performance of several geometric transformation models applied to image matching techniques in planetary DTM reconstruction. A general purpose matching software (DM) developed by the University of Parma was compared with Ames Stereo Pipeline developed at NASA. It turned out that using similar (though not identical) matching techniques (NCC or affine warping), they basically achieve the same results. However, in the comparison of DTMs from HiRISE and LROC NAC images with reference data, systematic errors are still present (see Figure 4 and 10) as repetitive pattern. The reason might be due to effects on the DTM reconstruction of different preprocessing of image data and/or different values of orientation data that are not removed by the rigid alignment performed before the comparison. All tests showed that the best results are achieved with quite large templates: more than 15 pixel for AFF models and more than 23 pixel for higher order transformation models (PROJ and POLY). The use of higher order geometrical models did not improve significantly the accuracy of the results, though involving much longer computing time. Our guess is that probably such models can outperform AFF only with smooth curved surfaces (like the one used in [11]), while with rough terrain (rocks, steep ridges, etc.) even POLY cannot model the ground shape effectively. The issue should be investigated thoroughly and an adaptive matching algorithm that can switch between transformation models according to the ground shape features, or a filter that selectively find those pixels where discontinuities arise should be developed. Finally it's worth noting that the NCC algorithm with appropriate image preprocessing in many circumstances reaches in practice the same accuracy of more complex models, but with a computational effort that can be an order of magnitude or more lower. A deeper understanding of the error budget (i.e. the contribution of every error source: navigation parameters, interior orientation, image artifacts, etc.) and the influence of the matching algorithm used would point to where to focus future improvements in the workflow.

7. ACKNOWLEDGMENTS

This research has made use of the USGS Integrated Software for Imagers and Spectrometers (ISIS) and of the ASP software. USGS, NASA, JPL and the University of Arizona are acknowledged for providing image and reference data.

This research is supported by the Italian Ministry of University and Research within the project "FIRB - Futuro in Ricerca 2010" – Subpixel techniques for matching, image registration and change detection and by the Italian Space Agency (ASI) within the SIMBIOSYS project (ASI-INAF agreement n. I/022/10/0).

REFERENCES

[1] Flamini E., et al., "SIMBIO-SYS: the spectrometer and imagers integrated observatory system for the BepiColombo planetary orbiter", Planet. Space Sci. 58, 125–143 (2010).

[2] Cremonese G., Fantinel D., Giro E., Capria M.T., Da Deppo V., Naletto G., Forlani G., Massironi M., Giacomini L., Sgavetti M., Simioni E., Bettanini C., Debei S., Zaccariotto M., Borin P., Marinangeli L., Flamini E., "The stereo camera on the BepiColombo ESA/JAXA mission: a novel approach", Advances in Geosciences 15, 305-322 (2009).

[3] Re C., Roncella R., Forlani G., Cremonese G., Naletto G., "Evaluation of area-based image matching applied to DTM generation with HiRISE images", ISPRS Annals of Photogrammetry, Remote Sensing and Spatial Information Sciences, Vol I-4, 209-214 (2012).

[4] Grün A. "Adaptive least squares correlation - a powerful image matching technique". South African J. Photogramm. Remote Sensing and Cartography, 14(3), 175-187 (1985).

[5] Massironi M. et al. "Simulations using terrestrial geological analogues to asses interpretability of potential geological feature of the Hermean surface restituted by the STereo imaging Camera of the SIMBIO-SYS package (BepiColombo mission)". Planetary and Space Science 56, 1079–1092 (2008).

[6] McEwen. A et al. "Mars Reconnaissance Orbiter's High Resolution Imaging Science Experiment (HiRISE)". J. Geophysical Research, Vol. 112, E05S02, 40 pp (2007).

[7] Robinson M.S. et al., "Lunar Reconnaissance Orbiter Camera (LROC) Instrument Overview", Space Science Reviews, Volume 150, Issue 1-4, 81-124 (2010).

[8] Broxton, M. J., Edwards, L. J. "The Ames Stereo Pipeline: Automated 3D Surface Reconstruction from Orbital Imagery". Lunar and Planetary Science Conference 39, abstract #2419, (2008).

[9] Zitová B., Flusser J. "Image registration methods: a survey". Image and Vision Computing 21 (2003), 977–1000 (2003).

[10] W.K. Pratt, Digital Image Processing, 2nd ed., Wiley, New York, (1991).

[11] Bethmann F., Luhmann T. "Least-squares matching with advanced geometric transformation models". International Archives of Photogrammetry, Remote Sensing and Spatial Information Sciences, Vol. XXXVIII, Part 5 Commission V Symposium, Newcastle upon Tyne, UK., 86-91 (2010).

[12] Grün A., Baltsavias E.P. "Geometrically constrained multiphoto matching". *PE&RS*, 54(5), 633-641 (1988).

[13] Bay, H. et al. "SURF: Speeded Up Robust Features". *CVIU*, Vol. 110, No. 3, 346-359 (2008).

[14] Moratto, Z., Broxton, M.J., Beyer, R.A., Lundy, M., Husmann, K. "Ames Stereo Pipeline, NASA's Open Source Automated Stereogrammetry Software". Lunar and Planetary Science Conference 41, abstract #2364, (2010).

[15] Torson, J.M., and Becker, K.J., "ISIS - A Software Architecture for Processing Planetary Images" (abs.), Lunar and Planetary Science Conference 38, 1443-1444 (1997).

[16] Broxton M. J. et al. "The Ames Stereo Pipeline: NASA's Open Source Automated Stereogrammetry Software". v. 1.0.5. <http://ti.arc.nasa.gov/m/project/ngt/asp_book_1.0.5.pdf> (10 January 2012).